Evidence for double injections in scatter-free solar impulsive electron events

L. Wang,[1,2] R. P. Lin,[1,2] S. Krucker,[1] and J. T. Gosling[3]

Received 19 August 2005; revised 13 December 2005; accepted 30 December 2005; published 10 February 2006.

[1] We investigate the injection at the Sun for three scatter-free impulsive electron events (7 August 1999, 28 June and 22 August 2000) observed from ~0.4 to 300 keV by the WIND 3DP instrument. Taking into account the interplanetary scatter-free propagation and instrumental effects, we find that the observed time profiles of electron fluxes at all energies fit well to triangular injections at the Sun with equal rise and fall times. We find two distinct injections: that of ~0.4 to 6–9 keV electrons begins 9.1 ± 4.7 min before the start of the type III radio burst and lasts for 50–300 min, while that of ~13 to 300 keV electrons starts 7.6 ± 1.3 min after the start of the type III burst and lasts for a factor of 5–10 times shorter. Electrons of the low-energy injection are likely to be the source of the type III radio bursts, and the delayed high-energy injection occurs when the associated CME passes altitudes of ~1–6 $R_\odot$. The observed electron energy spectra fit to double power-law with a downward break at ~40–50 keV, but exhibit a smooth power-law across the transition (~6–13 keV) between the two injections, suggesting the low-energy injection may provide the seed electrons for the high-energy injection. **Citation:** Wang, L., R. P. Lin, S. Krucker, and J. T. Gosling (2006), Evidence for double injections in scatter-free solar impulsive electron events, *Geophys. Res. Lett.*, *33*, L03106, doi:10.1029/2005GL024434.

1. Introduction

[2] Solar impulsive electron events (see *Lin* [1985] for review) were first observed above ~40 keV with fast rise-slow decay temporal profiles indicative of significant scattering in the interplanetary medium (IPM). Later, events were detected down to keV energies (and even ~0.1 keV [*Gosling et al.*, 2003]), occasionally with fast rise-fast decay profiles that imply essentially scatter-free propagation in the IPM [*Lin*, 1974]. Near solar maximum, $\gtrsim 10^2$ events/month occur over the whole Sun. They are often accompanied by low-energy, ~MeV/nucleon ion emissions that are highly enriched in ^{3}He [*Reames et al.*, 1985]. These electron/^{3}He-rich events form the class of "impulsive" solar energetic particle (SEP) events. For about 90% of impulsive electron events observed near 1 AU by ISEE-3, a type III solar radio burst was detected within 20 min.

[3] Using WIND observations, *Krucker et al.* [1999] found the injection of the >25 keV electrons were often delayed by of order ~10 min after the type III radio burst at the Sun, and suggested the delays may be related to propagation of large-scale coronal transient (EIT or Moreton) waves. *Haggerty and Roelof* [2002] found a median delay of ~10 min for 38–315 keV electrons; they and *Simnett et al.* [2002] suggested acceleration by shock waves associated with coronal mass ejections (CMEs). *Maia and Pick* [2004] and *Klein et al.* [2005] proposed that these events are related to the coronal magnetic restructuring in the aftermath of CMEs, while *Cane and Erickson* [2003] and *Cane* [2003] argued from radio observations that the electrons are injected simultaneously with the type III burst, and that the delays are due to propagation effects in the IPM.

[5] With WIND electron observations from ~0.4 to 300 keV, we infer the solar injection profile for three electron events that have strongly scatter-free time profiles. We find evidence for double injections: one for ~0.4 to ~6–9 keV electrons that begins early enough to account for the type III burst, and a second for electrons above ~10–13 keV that starts ~8 min after the type III burst.

2. Observations and Data Analysis

[6] The 3-D Plasma and Energetic Particle (3DP) instrument on WIND provides full three-dimensional measurements of electron distributions [*Lin et al.*, 1995], utilizing silicon semiconductor telescopes (SST) and electron electrostatic analyzers (EESA-L and EESA-H) to measure ~20–400 keV and ~3 eV–30 keV electrons with energy resolution of $\Delta E/E \approx 0.3$ and 0.2, respectively, all with angular resolution of ~22.5°.

[7] From Haggerty and Roelof's list of delayed >38 keV electron events, we selected three events - 7 August 1999, 28 June and 22 August 2000 - with strongly scatter-free temporal profiles that were observed by WIND/3DP from ~0.4 to 300 keV. Figure 1 shows the outward-traveling electron fluxes versus time from ~0.4 to 310 keV (channel center energies) for the 7 August 1999 event. The temporal profiles at all energies exhibit nearly symmetric rapid-rise, rapid-decay peaks, followed by slow decays at flux levels much lower than the peak values. Such profiles imply that most of the electrons (those in the peak) propagated through the IPM essentially scatter-free [*Lin*, 1974], and that the injection at the Sun was impulsive and nearly symmetric. The electron pitch angle distributions (not shown) are strongly peaked along the magnetic field through the rapid-rise, rapid-decay phase, with the half maximum of $\lesssim 30°$ at $\lesssim 1$ keV up to ~50° at $\gtrsim 100$ keV.

[1] Space Sciences Laboratory, University of California, Berkeley, California, USA.
[2] Also at Physics Department, University of California, Berkeley, California, USA.
[3] Laboratory for Atmospheric and Space physics, University of Colorado, Boulder, Colorado, USA.

0094-8276/06/2005GL024434

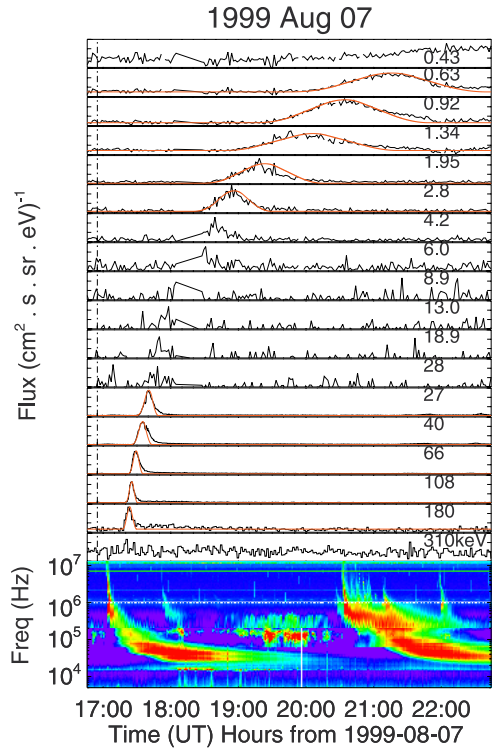

Figure 1. Overview plot for the 7 August 1999 event. The top panels show the flux of electrons traveling parallel to the magnetic field direction (outward) on a linear scale: observations (black curves) by EESA-H (0.43–28 keV) and by SST (27–310keV), and best fits (red curves) superimposed on the pre-event background. A data gap occurred in the interval from 1804 to 1827 UT in the energy channels of EESA-H. The bottom panel shows a radio spectrogram observed by the WIND/WAVES experiment. A type III radio burst was observed with an Earth-observed onset at 1703 UT (the solar onset is indicated by dash line in the top panels). Langmuir plasma waves (thin line at ~17 kHz) were detected from ~1805 to 1920 UT.

[8] Velocity dispersion is clearly evident from ~0.4 to 310 keV. For electrons above ~25 keV, the times, t_i, of the peak fluxes at different velocities, v_i, fit well to a straight line, $L = v_i[t_i - t_0]$, implying a simultaneous solar injection at these energies followed by travel along the same path of length $L = 1.19 \pm 0.14$ AU (about the 1.13 AU smooth spiral field length for the observed solar wind speed of 450 km/s). Using the observed onset at 180 keV (after correcting for contamination of lower-energy channels due to higher-energy electrons scattering out of the silicon detectors and depositing only part of their energy) and this path length, we find ~1703 UT as the earliest electron release time at the Sun. The solar type III radio burst (bottom of Figure 1) observed by the Wind/WAVES instrument (12 MHz to ~20 kHz), and by ground observatories up to ≳80 MHz, left the Sun at ~1655 UT (dash line). Thus, the injection of electrons above 25 keV is delayed by ~8 min after the type III burst injection. No Hα flare or GOES soft X-ray (SXR) burst were reported at this time in Solar-Geophysical Data. Langmuir waves at the local plasma frequency (~17 kHz) were observed from

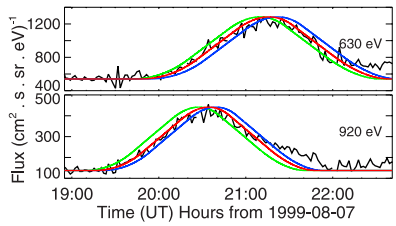

Figure 2. Examples of error analysis for two energy channels: (top) 630 eV and (bottom) 920 eV. The red curves are the best fits to the rise of in situ electron flux profiles (black curves). The green and blue curves are the upper and lower limits of fitting, respectively.

1805 to ~1920 UT (Figure 1, bottom), during the rise of the ~1.34 to ~8.9 keV electron fluxes.

[9] Based on electron observations of Figure 1, we assumed the injection flux at the Sun was an isosceles triangle-shaped pulse $f(E, t_0(E), \Delta t(E), A, t)$:

$$f = \begin{cases} A \cdot E^{-\beta} \cdot \left(1 - \dfrac{|t - t_0 - \Delta t/2|}{\Delta t/2}\right) & 0 \le t - t_0 \le \Delta t; \\ 0 & \text{otherwise,} \end{cases}$$

where $t_0(E)$ and $\Delta t(E)$ are the start time and the time duration of electron injection at energy E; $A \cdot E^{-\beta}$ represents the injection flux intensity, and β is the index of electron peak flux spectrum observed at 1 AU. Assuming that the propagation is scatter-free without energy losses (to be discussed later), and $t_0(E) = t_{0j}$, $\Delta t(E) = \Delta t_j$ and $A = A_j$ within the energy band (from E_{j-} to E_{j+}) of the channel j, we find that the electron flux F_j at the propagation distance L from the Sun is:

$$F_j(L,t) = \frac{\int_{E_{j-}}^{E_{j+}} f\left(E, t_{0j} + \dfrac{L}{v(E)}, \Delta t_j, A_j, t\right) dE}{E_{j+} - E_{j-}}$$

where $v(E)$ is the electron speed. The solar injection pulse $F_j(0, t)$ is determined by fitting $F_j(1.2AU, t)$ to the observed electron flux profile for energy channel j, varying the start time t_{0j}, the duration Δt_j and the intensity A_j.

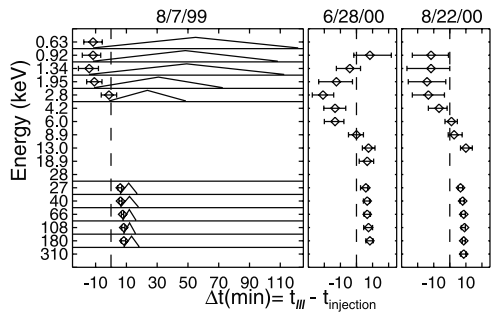

Figure 3. Comparison of the start times of inferred electron injections at different energies (diamonds) and the release time of type III burst (dash line) at the Sun for the three events. The electron delay (X-axis) is shown in min. For the 7 August 1999 event (left), the inferred injection profiles are shown by triangles. The injection analysis was not available at some channels due to a data gap or poor statistics.

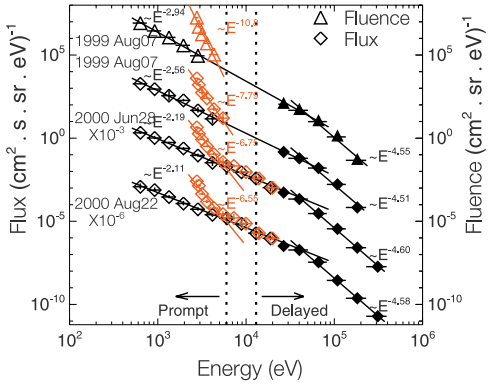

Figure 4. Background-subtracted peak flux spectra (EESA-H open symbols; SST solid symbols) for the three events and fluence spectrum for the 7 August 1999 event: in situ spectra (black) and source spectra (red; not shown above 20 keV). The spectra of the two events in 2000 have been multiplied by 10^{-3} and 10^{-6}, respectively. The dotted vertical lines indicate the transition (∼6–13 keV) between electrons with prompt and delayed injections with respect to type III radio emissions.

[10] For the 7 August 1999 event, this analysis was applied to energy channels from 0.63 to 180 keV, excluding 4.2 to 18.9 keV because of a data gap or poor statistics. The fits (shown as red curves in Figures 1 and 2) are generally very good through the rapid-rise, rapid-fall phase. Afterward, the observed electron fluxes show a much slower decay and the angular distributions become broader, as expected from scattering in the IPM. The corresponding injection profiles are shown as triangles in the left panel of Figure 3.

[11] The uncertainties in the start-time of the injection $F_j(0, t)$ were estimated from the fit of $F_j(1.2AU, t)$ to in situ observations, as shown in Figure 2 for the 630 and 920 eV channels. The green and blue curves were chosen as upper and lower limits of fitting to the rise of in situ electron flux profiles; the limits on the start times of the corresponding $F_j(0, t)$ are shown as error bars on the injection time in Figure 3.

[12] Figure 3 (left) shows that electron injections above ∼27 keV have short durations (∼8–12 min) and clearly delayed starts (7.3 ± 1.2 min) relative to the coronal release time of the type III radio burst (dash line), while electron injections below ∼3 keV start 9.9 ± 5.8 min before the type III burst and have much longer durations (∼50–130 min).

[13] The 28 June and 22 August events in 2000 have similar scatter-free time profiles, and the same triangular injection analysis was applied. In the 28 June event, a 1.12 ± 0.17 AU path length is obtained from the velocity dispersion analysis of the peak flux times for the high-energy (>25 keV) channels. About two hours after the onset, an increase in fluxes occurred simultaneously at all energies, suggesting that the magnetic connection to the Sun had changed. In the 22 August event a second injection occurred ∼15–20 min after the first, and the in situ peaks were separable only at energies above 100 keV. The dispersion analysis of those peak times gives 1.33 ± 0.95 AU and 1.15 ± 0.70 AU path lengths for the two injections. Both events show some back-streaming electrons due to magnetic connection to the Earth's bow shock. Thus, the triangular injections for these events were constrained almost entirely by the fits to the rise to maximum, especially at the lower energies.

[14] Solar type III radio bursts were observed by WIND/WAVES up to 12 MHz and by ground measurements (∼80–170 MHz) for both events. A coronal type II burst (>20MHz) was reported for the 28 June event, and possibly for the 22 August event (uncertain emissions). Also GOES C2.5 and C3.7 SXR bursts were associated with these events, respectively, but no Hα flares were reported. The SOHO/EIT difference images show flaring on, or partly behind, the western limb for the 28 June event.

[15] Figure 3 (right) shows that electrons above ∼9–13 keV are injected with a median delay of 7.8 ± 1.8 min after the coronal release of type III radio bursts, while electrons below ∼6–9 keV are injected 8.7 ± 6.4 min earlier than type III bursts. The durations (not shown) range from ∼30 and 15–30 min for energies above ∼30 keV, to 230–300 and 230–300 min below ∼3 keV, for the 28 June and 22 August events, respectively. In situ Langmuir waves were observed during the onset of the ∼1–13 keV electrons for both of these events as well.

[16] Figure 4 shows in situ background-subtracted electron spectra (black) for the three events, constructed by taking the maximum outward flux in each energy channel. For the 7 August 1999 event, the in situ fluence spectrum (black), obtained by integrating the net outward flux over the event duration in each energy channel, is also shown. All of the spectra fit to a double power-law with exponents of 2.1–2.6 (2.9 for the fluence spectrum) below the break (∼40–50 keV) and 4.5–4.6 above. There is no obvious change in the in situ spectra across the transition between the early injection (≲6–9 keV) and late injection (≳13 keV) electrons. For the 7 August 1999 event, the fluence spectrum is softer below the break but has the same exponent above the break, compared with the peak flux spectrum, likely due to the longer durations at lower energies.

3. Discussion

[17] By taking into account the effects of interplanetary propagation and instrument response in these highly scatter-free events, we have shown that there are double impulsive electron injections at the Sun: a low-energy (∼0.4 to 6–9 keV) injection that begins 9.1 ± 4.7 min earlier than the type III radio bursts and lasts for ∼50–300 min, and a high-energy (10–13 to 300 keV) injection that starts 7.6 ± 1.3 min after the type III bursts but has durations ∼5–10 times shorter. (e.g., triangles in Figure 3). The source of the type III radio burst can be identified with the low-energy electron injection; some delay is needed for the injected electrons to rise above the ambient background plasma to produce the significant positive slopes in the electron reduced parallel velocity distribution function required for the growth of the Langmuir waves that, in turn, scatter to produce the type III radio emission at the fundamental and harmonic of the plasma frequency (see *Lin* [1990] for summary). This is

also consistent with the detection of Langmuir waves in situ when the ~1–10 keV electrons arrive near 1 AU in these events and previous events [*Ergun et al.*, 1998], and with the drift rate of decametric type III bursts indicating exciter speeds of ~0.1 c [*Haggerty and Roelof*, 2002].

[18] For all three events the associated type III radio bursts start at frequencies ≳80 MHz, implying that the injection occurs at coronal densities of $\gtrsim 10^8$ cm^{-3}, corresponding to an overlying column depth of $\sim 10^{18}$ cm^{-2} and ~0.1–0.2 $R_\odot$ altitude for a quiet-Sun model [*Saito et al.*, 1977]. Electrons escaping from there will lose energy to Coulomb collisions and to the ambipolar electrostatic potential that results from the fact that coronal ions are gravitationally bound while hot coronal electrons are not: $dE/dr = (dE/dr)_{Coll} + (dE/dr)_{AEP}$. The Coulomb collision term in ionized hydrogen [*Trubnikov*, 1965] can be estimated as: $(dE/dr)_{Coll} = -1.82 \times 10^7 n_i(r)/E$, where E is the electron energy in keV, r is the radial distance from the Sun center in $R_\odot$, and n_i is the hydrogen density in cm^{-3}. The electrostatic potential term in hydrostatic equilibrium [*Lemaire and Scherer*, 1973] can be written: $(dE/dr)_{AEP} = -0.994/r^2$. A ~0.4 keV electron detected at 1 AU thus begins as a ~2.6–3.2 keV electron in the metric type III source region. The resultant change on inferred solar injection times is small (e.g., ~160 s for 630 eV and ~1 s for 18.9 keV) compared to the difference in injection times of low-energy electrons, high-energy electrons and type III bursts. This result is, of course, model-dependent; to our knowledge, the interplanetary potential has never been measured directly.

[19] We can obtain the electron source spectrum by assuming a constant flow: $S_0 \cdot J_{0n} \cdot \Delta E_{0n} = S_1 \cdot J_{1n} \cdot \Delta E_{1n}$, where J_{0n} (J_{1n}) is the flux of channel n, ΔE_{0n} (ΔE_{1n}) is the energy bandwidth and S_0 (S_1) is the cross-sectional area at the Sun (at 1 AU). For all three events, the resultant fluxes (fluences) and energies at the Sun are shown in red in Figure 4. Using an active coronal density model would change the altitude of the source region, but the power-law indices of the source spectra would only change by ≲10%. Above ~10 keV, the source spectra is essentially the same as the spectra measured in situ at 1 AU. Below ~6 keV, the source spectra breaks upward with a steep power-law for all three events (indices of ~6.5–11). It is surprising that these energy loss processes, however, would be just what is required to produce a power-law below 6 keV that matches the power-law above 6 keV, as observed.

[20] For the delayed high-energy electron injection, recent studies suggested acceleration by some propagating phenomena such as EIT waves and their coronal counterparts [*Krucker et al.*, 1999], or upward moving shocks driven by CMEs [*Haggerty and Roelof*, 2002; *Simnett et al.*, 2002]. All three events had associated west-limb CMEs (SOHO/LASCO CME Catalog compiled by Yashiro); the CME speeds and angular widths were ~570 km/s and ~7° for the 1999 event, and >950 km/s and >100° for the two events in 2000. From the CME height-time plots, we find that for the 1999 event, the CME is at ~1–2 $R_\odot$ altitude when the high-energy electrons are injected, and for the two events in 2000, the projected altitudes are ~2–6 $R_\odot$ and ~2–5 $R_\odot$. By the time the prompt electrons reach those altitudes, they will have already suffered most of their energy losses so their spectra will be similar to the spectra observed at 1 AU. The relatively smooth transition across the transition energy range suggests that the prompt electrons may provide the seed particles for the delayed electron acceleration.

[21] The inferred low-energy injections at the Sun have durations of from ~50 min to several hours. This is consistent with the finding that many electron events at energies of ~0.1–1.4 keV have a beam duration >3 hours [*Gosling et al.*, 2003]. Simple calculations show that pitch-angle scattering and dispersion in the IPM might only cause an error of ≲10% in the determination of time duration for highly scatter-free events. Thus, these long durations are unlikely to be due to propagation in the IPM. If the acceleration is rapid but the electrons are temporarily stored in the corona and gradually released, the injection spectrum should harden with time since lower-energy electrons lose energy to Coulomb collisions more rapidly than higher-energy ones. For the 7 August 1999 event, however, the spectrum of the derived injection profiles softens with time. On the other hand, near-Sun radio/X-ray observations do not show evidence for long-lived (≳hour) electron acceleration, e.g., no long-duration radio or X-ray emission.

[22] The start time of the prompt low-energy electron injection occurs close to the start of the CME eruption, as extrapolated from the height-time plots. Thus, one possibility is that the low-energy injection and type III burst may be related to the initial CME eruption, with the injection continuing as the corona restructures while the CME continues outward [*Maia and Pick*, 2004; *Klein et al.*, 2005]. The delayed high-energy injection may be related to a propagating shock (although it may be difficult to explain the short injection duration of high-energy electrons) or other phenomena whose formation/start is delayed relative to the CME initiation, with the acceleration acting on the seed low-energy electrons. The 7 August 1999 and 22 August 2000 events were both associated with strongly ^{3}He-rich solar energetic ion events (G. Mason, private communication, 2004). The 28 June 2000 event was not ^{3}He-rich, and it had an associated type II radio burst, indicating it is likely a gradual event while the other two events are impulsive events.

[23] **Acknowledgments.** We thank Hugh Hudson for helpful discussions, G. Mason for information on the ion composition, and the WAVES team on WIND for sharing data with us. This research at Berkeley is supported by NASA grant NNG05GH18G. J.T. Gosling is supported by NASA grant NNG05GJ55G.

References

Cane, H. V., and W. C. Erickson (2003), Energetic particle propagation in the inner heliosphere as deduced from low-frequency (<100 kHz) observations of type III radio bursts, *J. Geophys. Res.*, *108*(A5), 1203, doi:10.1029/2002JA009488.

Cane, H. V. (2003), Near-relativistic solar electrons and type III radio bursts, *Astrophys. J.*, *598*, 1403.

Ergun, R. E., et al. (1998), Wind spacecraft observations of solar impulsive electron events associated with solar type III radio bursts, *Astrophys. J.*, *503*, 435.

Gosling, J. T., et al. (2003), Solar electron bursts at very low energies: Evidence for acceleration in the high corona?, *Geophys. Res. Lett.*, *30*(13), 1697, doi:10.1029/2003GL017079.

Haggerty, D. K., and E. C. Roelof (2002), Impulsive near-relativistic solar electron events: Delayed injection with respect to solar electromagnetic emission, *Astrophys. J.*, *579*, 841.

Klein, K.-L., et al. (2005), Coronal phenomena at the release of solar energetic electron events, *Astron. Astrophys.*, *431*, 1047.

Krucker, S., et al. (1999), On the origin of impulsive electron events observed at 1 AU, *Astrophys. J.*, *519*, 864.

Lemaire, J., and M. Scherer (1973), Kinetic models of solar and polar winds, *Rev. Geophys.*, *11*, 427.

Lin, R. P. (1974), Non-relativistic solar electrons, *Space Sci. Rev.*, *16*, 189.

Lin, R. P. (1985), Energetic solar electrons in the interplanetary medium, *Sol. Phys.*, *100*, 537.

Lin, R. P. (1990), Electron beams and Langmuir turbulence in solar type III radio bursts observed in the interplanetary medium, in *Basic Plasma Processes on the Sun*, edited by E. R. Priest and V. Krishnan, p. 467, Int. Astron. Union, Netherlands.

Lin, R. P., et al. (1995), A three-dimensional plasma and energetic particle investigation for the Wind spacecraft, *Space Sci. Rev.*, *71*, 125.

Maia, D., and M. Pick (2004), Revisiting the origin of impulsive electron events: Coronal magnetic restructuring, *Astrophys. J.*, *609*, 1082.

Reames, D. V., et al. (1985), Solar 3He-rich events and nonrelativistic electron events: A new association, *Astrophys. J.*, *292*, 716.

Simnett, G. M., et al. (2002), The acceleration and release of near-relativistic electrons by coronal mass ejections, *Astrophys. J.*, *579*, 854.

Saito, K., et al. (1977), A study of the background corona near solar minimum, *Sol. Phys.*, *55*, 121.

Trubnikov, B. A. (1965), Particle interactions in a fully ionized plasma, *Rev. Plasma Phys.*, *1*, 105.

J. T. Gosling, Laboratory for Atmospheric and Space Physics, University of Colorado, 1234 Innovation Drive, Boulder, CO 80303, USA.

S. Krucker, R. P. Lin, and L. Wang, Space Sciences Laboratory, University of California, Berkeley, CA 94720, USA. (windsound@ssl.berkeley.edu)